Luiza Kondaurova
Institute of Thermophysics, Novosibirsk, Russia

Overview of theoretical and experimental investigations of the stationary case of Vinen’s equation

1. Equations for vortex line density evolution. Vinen’s equation

2. Hydrodynamics of superfluid turbulence

3. Experiments and simulations on quantum turbulence

The understanding of coupled dynamics of superfluid and normal fluid we get usually from:

- Experiments
- Theory
- Simulations

a) The hydrodynamic equations of superfluid turbulence (HST) are used for description of heat transfer processes in applications and dynamics of nonlinear waves of second sound.

The structure of the vortex tangle is not considered. The new hydrodynamic variable (density of the vortex tangle) is introduced. Equation for the density of the vortex filaments is included in the HST system

b) Many researchers use a 'vortex filament method' to describe the experimental observations of some macroscopic and statistical properties of the vortex tangle. Usually, the calculations are performed for a given velocity profile of the normal component

Vinen's equation

W.F. Vinen, Proc. R. Soc. London, Ser. A **240**, 128 (1957),
Proc. R. Soc. London, Ser. A **242**, 493 (1957)

Vinen's equation was obtained in the framework described by R.P. Feynman, Progress in Low Temperature Physics Vol. I (1955), p.17

$$\frac{dL(t)}{dt} = \left[\frac{dL}{dt}\right]_{gen} - \left[\frac{dL}{dt}\right]_{dec} = \frac{\chi_1 B \rho_n |\mathbf{v}_{ns}|}{\rho} L^{3/2} - \frac{\chi_2 \kappa}{2\pi} L^2 = \alpha_V |\mathbf{v}_{ns}| L^{3/2} - \beta_V L^2$$

α_V , β_V - are parameters of Vinen's theory

$$\frac{dL}{dt} = 0 \Rightarrow L^{1/2} = \gamma_V \mathrm{v}_{\mathrm{ns}}, \quad \gamma_V = \frac{\pi B \rho_n \chi_1}{\kappa \rho \chi_2}$$

Vinen's relation

In the same paper Vinen suggested that the form of the first term may be different.

$$\frac{dL(t)}{dt} = \alpha_{alt} |\mathbf{v}_{ns}|^2 L - \beta_{alt} L^2$$

W.F. Vinen, Proc. R. Soc. London, Ser. A **242**, 493 (1957)

Schwarz's equation

K.W. Schwarz, Phys. Rev. Lett. **38**, 551 (1977); Phys. Rev. B **18**, 245 (1978); Phys. Rev. Lett. **49**, 283 (1982); Phys. Rev. B, **38,** 2398 (1988); K.W. Schwarz and J.R. Rozen, Phys. Rev. B, **44,** 7563 (1991)

$$\frac{dL}{dt} = \alpha I_l \left|\mathbf{v}_{ns}\right| L^{3/2} - \alpha\beta c_2^2 L^2$$

$$I_l = \frac{l}{L_{tot}} \int_c \hat{r}_{II} \cdot \left(s' \times s''\right) d\zeta$$

$l = 1/\sqrt{L}$, L_{tot} – the total length of lines

$\hat{r}_{II}$ – a unit vector parallel to $\mathbf{v}_{ns}$

$$\gamma_S = c_L / \beta$$

$$c_L = I_l / c_2^2$$

$$c_2 = \tilde{S} / \sqrt{L}$$

$$\tilde{S}^2 = \left\langle \left|s''\right|^2 \right\rangle = \frac{1}{L_{tot}} \int_C \left|s''\right|^2 d\xi$$

$$\beta = \kappa\tilde{\Lambda} \approx \ln\left[l / a_0\right] / 4\pi \approx 1$$

Schwarz obtained the equation for the L(t), starting from first principles i.e., from the dynamic equations of motion. The obtained equation is in agreement with the form of Vinen's equation.

Note that according to Schwarz's theory the decreasing of vortex line length is caused by friction force. According to Feynman-Vinen theory, the decreasing of vortex line length is caused by breaking of a large vortex into smaller vortices like the cascade processes in classical turbulence.

Equations for vortex line density evolution

A vortex tangle is not isotropic in a counterflow channel. Several ways have been proposed to modify Vinen's equation in more general situations.

D. Khomenko, L. Kondaurova, V.S. L'vov, P. Mishra, A. Pomyalov, and I. Procaccia, Phys. Rev. B, **91**, 180504 (2015)

$$\frac{\partial L(r,t)}{\partial t} + \nabla \cdot J_{cl}(r,t) = C_1 \left| \mathbf{v}_{ns} \right|^3 \sqrt{L} - \beta L^2$$

$$J_{cl}(r,t) = -C_{flux} (\alpha / 2\kappa) \nabla^2 \mathbf{v}_{ns}$$

J.A. Geurst, Physica A, **183**, 279 (1992).

$$\frac{\partial L(r,t)}{\partial t} + div(L\mathbf{v}_L) = \varepsilon a_G \left| \mathbf{v}_n - \mathbf{v} \right| L^{3/2} - \beta_G L^2$$

$$\varepsilon = \mathrm{sgn}(\mathbf{v}_L - \mathbf{v})\,\mathrm{sgn}(\mathbf{v}_n - \mathbf{v}),\ \mathbf{v} \text{ is average mass velocity}$$

K.W. Schwarz, Phys. Rev. B, **38,** 2398 (1988);
S.K. Nemirovskii, Phys. Rev. B, **57,** 5972 (1998);
T. Lipniacki, Phys. Rev. B, **64,** 214516 (2001);
D. Jou, M.S. Mongiovi, M. Sciacca, Physica D, **240**, 249 (2011).

Hydrodynamics of superfluid turbulence (HST)

A change of the hydrodynamic characteristics leads to an immediate change of the *L* and vice versa. Therefore the study (by hydrodynamic means) of superfluid turbulence and the study of hydrodynamic processes in the presence of a vortex tangle are indivisible parts of one general problem. The form of the hydrodynamic equations depends on the type of turbulence. Here we will consider the case of the counterflowing (Vinen) turbulence.

- S. Nemirovskii, V. Lebedev, Sov. Phys. - JETP **84,** 1729 (1983); J. Low Temp. Phys., **113**, 591 (1998). Phenomenological method of constructing HST
- K. Yamada, S. Kashiwamura, K. Miyake, Physica B,(ISSN:0921-4526), **154**, 318 (1989). HST equations based on the microscopic, Schwarz kinetic theory. Yamada's et al. formulation is based on the Langevin stochastic equation and the use of the Fokker-Plank equation.
- J. Gerst, Physica A, **183**, 279 (1992). The HST equations were deduced for the case of one dimensional flow from a variational principle.

Phenomenological method of constructing HST

Dynamics of vortex tangle density + the classical two fluid Landau Khalatnikov hydrodynamic equations

S.K. Nemirovskii, V.V. Lebedev, Sov. Phys.-JETP **84,** 1729 (1983);
J. Low Temp. Phys., **113**, 591 (1998).

$$\frac{\partial S}{\partial t} + div\left(S\mathbf{v}_n\right) = \frac{1}{T}\left(\alpha_1 L \mathbf{v}_{ns}{}^2 + \varepsilon_\beta \beta L^2\right)$$

$$\frac{\partial \mathbf{v}_s}{\partial t} + \nabla\left(\mu\left(p,\sigma,\mathbf{v}_{ns}\right) + \frac{\mathbf{v}_s^2}{2}\right) = \frac{\alpha_1 L}{\rho_S}\mathbf{v}_{ns} + \frac{\varepsilon_\beta \alpha}{\rho_S} L^{3/2}\frac{\mathbf{v}_{ns}}{\left|\mathbf{v}_{ns}\right|}$$

$$\frac{\partial \mathbf{j}_i}{\partial t} + \frac{\partial\left(\pi_{ik} + \tau_{ik}\right)}{\partial x_k} = 0$$

$$\frac{\partial \rho}{\partial t} + div\mathbf{j} = 0$$

$$\frac{\partial L}{\partial t} + div\left(\mathbf{v}_L L\right) = \chi_1 \frac{B\rho_n}{\rho}\left|\mathbf{v}_{ns}\right| L^{3/2} - \chi_2 \kappa L^2$$

$$S = \sigma\rho$$

$$\mathbf{v}_{ns} = \mathbf{v_n} - \mathbf{v_s}$$

$$\rho = \rho_n + \rho_s$$

$$\kappa = h / m_{He}$$

$$\sigma = \sigma_0 + \sigma, \quad T = T_0 + T$$

$$\sigma(p,T,\mathbf{v}_{ns}) = \sigma(p,T) + 1/2\mathbf{v}_{ns}{}^2 \partial\left(\rho_n / \rho\right)/\partial T$$

$$d\mu = -\sigma dT + dp/\rho - \left(\rho_n/\rho\right)\mathbf{v}_{ns} d\mathbf{v}_{ns}$$

$$\mathbf{j} = \rho_n \mathbf{v}_n + \rho_s \mathbf{v}_s = 0$$

$$\tau_{ik} = -\eta\left(\frac{\partial \mathbf{v}_{ni}}{\partial x_k} + \frac{\partial \mathbf{v}_{nk}}{\partial x_i} - \frac{2}{3}\delta_{ik}\frac{\partial \mathbf{v}_{nl}}{\partial x_l}\right) - \delta_{ik}\left[\xi_1 div\left(\mathbf{j} - \rho\mathbf{v}_n\right) + \xi_2 div\mathbf{v}_n\right]$$

$$\mathbf{j} = \rho_n \mathbf{v}_n + \rho_s \mathbf{v}_s, \quad \beta = \kappa\chi_2 / 2\pi, \quad \varepsilon_\beta = \rho_s \kappa^2$$

$$\pi_{ik} = \rho_n \mathbf{v}_{ni}\mathbf{v}_{nk} + \rho_s \mathbf{v}_{si}\mathbf{v}_{sk} + p\delta_{ik}, \quad \alpha = \chi_1 B\rho_n / 2\rho, \quad \alpha_1 = A\rho_s\rho_n\beta^2/\alpha^2$$

The HST equations taking into account the terms of the second order of smallness

L.P. Kondaurova, S.K. Nemirovskii, M.V. Nedoboiko, Low Temp. Phys., **25**, 639 (1999), J. of Low Temp. Phys. **119**, 329 (2000).

$$\frac{\partial T'}{\partial t}+\left[\frac{\rho_{s0}}{\rho}-\frac{\sigma_0}{\sigma_T}\frac{(\rho+\rho_n)}{\rho\rho_n}\frac{\partial\rho_n}{\partial T}\right]\mathbf{v}_{ns}\frac{\partial T'}{\partial x}+\frac{\rho_{s0}}{\rho}\left[\frac{\sigma_0}{\sigma_T}+\left(1-\frac{\sigma_{TT}\sigma_0}{\sigma_T^2}-\frac{\sigma_0}{\rho_{s0}\sigma_T}\frac{\partial\rho_n}{\partial T}\right)T'\right]\frac{\partial\mathbf{v}_{ns}}{\partial x}=$$

$$=-\frac{i\sigma_0\rho_{s0}}{\rho\sigma_T x}\mathbf{v}_{ns}-\frac{i}{\rho\sigma_T x}\left[\sigma_T\rho_{s0}-\frac{\sigma_0\sigma_{TT}\rho_{s0}}{\sigma_T}-\sigma_0\frac{\partial\rho_n}{\partial T}\right]T'\mathbf{v}_{ns}+\frac{1}{\rho\sigma_T T_0}\left(\alpha_1 L\mathbf{v}_{ns}{}^2+\varepsilon_\beta\beta L^2\right)$$

$$\frac{\partial\mathbf{v}_{ns}}{\partial t}+\left(\frac{3\rho_{s0}}{\rho}-\frac{\sigma_0\rho_s}{\sigma_T\rho\rho_n}\frac{\partial\rho_n}{\partial T}\right)\mathbf{v}_{ns}\frac{\partial\mathbf{v}_{ns}}{\partial x}+\frac{\rho}{\rho_n}\left[\sigma_0+\left(\sigma_T-\frac{\sigma_0}{\rho_n}\frac{\partial\rho_n}{\partial T}\right)T'\right]\frac{\partial T}{\partial x}=$$

$$=-\frac{\rho\alpha_1}{\rho_s\rho_n}L\mathbf{v}_{ns}-\frac{\rho\varepsilon_\beta\alpha}{\rho_s}L^{3/2}\frac{\mathbf{v}_{ns}}{|\mathbf{v}_{ns}|}$$

$$\frac{\partial L}{\partial t}-\frac{\rho_n}{\rho}L\frac{\partial\mathbf{v}_{ns}}{\partial x}-\frac{\rho_n}{\rho}\mathbf{v}_{ns}\frac{\partial L}{\partial x}=-\frac{i\rho_n\mathbf{v}_{ns}L}{\rho x}+\chi_1\frac{B\rho_n}{2\rho}|\mathbf{v}_{ns}|L^{3/2}-\frac{\chi_2 kL^2}{2\pi}$$

$$\sigma_T=\partial\sigma/\partial T,\quad \sigma_{TT}=\partial^2\sigma/\partial T^2,\quad V_L=V_s,\quad \mathbf{v}_{\rm ns}=\mathbf{v}_{\rm n}-\mathbf{v}_{\rm s}$$

i = 0, 1, 2 for the cases of plane, cylindrical and spherical geometry, correspondingly.
Discontinuity decay method (Godunov method), Numerical solution of multidimesional gasdynamic problem, S.K. Godunov, ed. (Nauka, Moscow, 1976).

Comparison of experimental data with calculations

The dynamics of periodic and single powerful heat pulses in various temperature regions where the coefficient of second sound nonlinearity takes a positive, negative and zero values were studied.

Kondaurova L.P., Nemirovskii S.K., Nedoboiko M.V., Cryogenics, **34**, 309 (1994); Chech.J.Phys., **46**, 23 (1996); J. Low Temp. Phys., **119**, 329 (2000); J. Low Temp. Phys., **150**, 200 (2008).

Experimens: W. Fiszdon, M.v. Schwerdtner, W. Poppe, J. Fluid Mech., **21**, 663 (1990).
The coefficient of second sound nonlinearity α_2 takes a positive value.

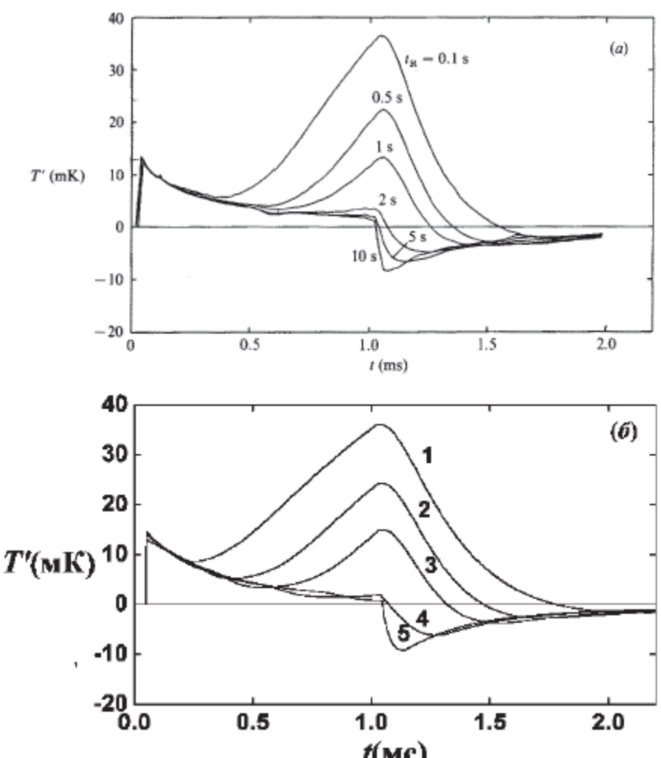

The time dependence of the temperature at a point located at a distance of 1 mm from the cylindrical heater. T = 1.4 K, Q = 4 W/cm^2, pulse duration 1ms, T_R is pulse repetition time.

a) experiments, b) results of our calculations

The quantitative agreement with experiment was obtained by increasing the value of the generating term in the Vinen equation in 1.5 times:

$$1.5 \cdot \chi_1 B \rho_n / 2\rho$$

Boiling times

The temperature attains the maximum values the near the heater, so the overheating and boiling of helium is possible. Depending on intensity of heating, two different experimental results an the time of boiling t_B as a function of the heat fluxes $Q^{\cdot}$ were observed (S.W.Van Sciver, Cryogenics, Plenum Press, 1986; S. Nemirovskii, A. Tsoi, Cryogenics **29** (1989) 985; R. Wang, Cryogenics **35**, 883 (1995); S.K. Nemirovskii, W. Fiszdon, Rev. Modern Phys. **67**, 37 (1995)).

$$Q^4 \cdot t_{boil} = B_{small}, \quad Q^2 \cdot t_{boil} = B_{large}$$

We got the time of boiling for small boiling heat fluxes when the vortex line density L takes its equilibrium value $L = \gamma^2 v^2_{ns}$.

Experimens: S.W. Van Sciver, Cryogenics **19**, 385 (1979)

$$Q^4 t_{boil} = B$$

$$T = 1.8K$$

$$B_{\exp} = 110 \left(W / cm^2\right)^4 \cdot c$$

$$B_{cul} = 80 \div 160 \left(W / cm^2\right)^4 \cdot c$$

$$T = 2.0K$$

$$B_{\exp} = 17 \left(W / cm^2\right)^4 \cdot c$$

$$B_{cul} = 49 \div 87 \left(W / cm^2\right)^4 \cdot c$$

The numerical results are in agreement with the experimental data considering scatter values of Gorter-Mellink constant at T=1.8 K. The obtained numerical results are not in agreement with the experimental data at T=2.0K

Required to know the equation of dynamics of vortex filaments, the value of Gorter-Mellink constant!

Experimental investigations of the stationary case of Vinen's equation

The vortex line density of the tangle can be easily determined by measuring then attenuation of second sound or from temperature differences.

Schematic view of the generation of counterflow turbulence of He II and its detection using second sound attenuation method.

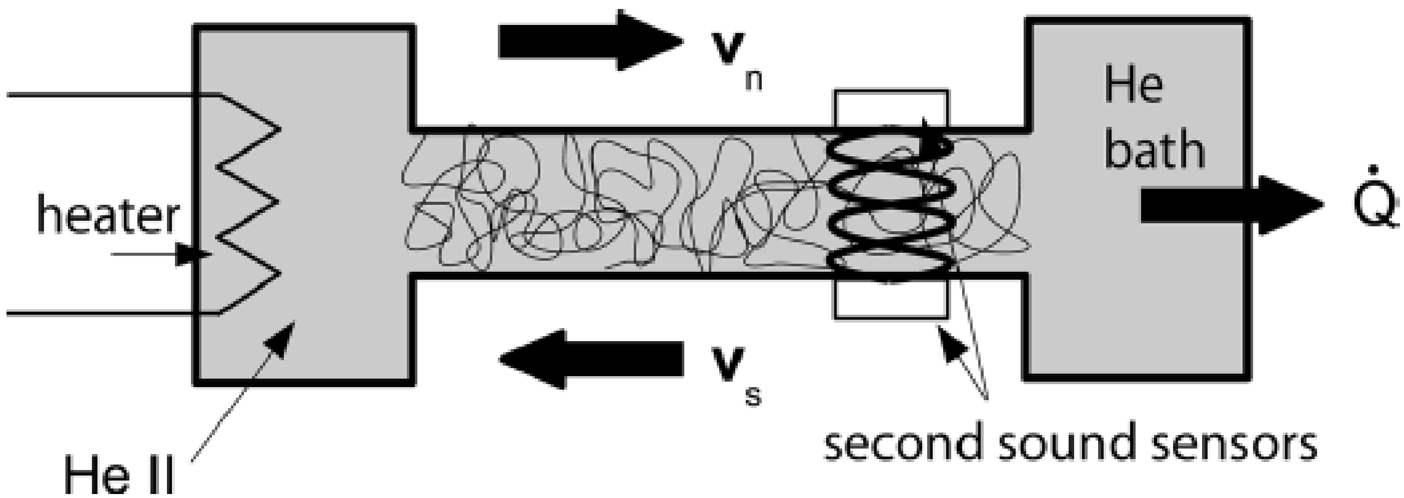

L. Skrbek and K.R. Sreenivasan, Physics of fluids **24**, 011301 (2012)

The experimental study of superfluid turbulence

γ varies greatly from experiment to experiment.

Vinen's relation: $L^{1/2} = \gamma_V \mathrm{v}_{ns}, \quad \gamma_V = \dfrac{\pi B \rho_n \chi_1}{\kappa \rho \chi_2}$

W.F. Vinen, Proc. Roy. Soc. London, Ser. A **240**, 114 (1957), and **243**, 400 (1957); counterflow in a 0.4 x 0.78 x 10 cm^3 wide, low-aspect-ratio rectangular metal channel.

V.P. Peshkov and V.J. Tkachenko, Zh. Eksp. Teor. Fiz. **41**, 1427 (1961) [Sov. Phys. - JETP **14**, 1019 (1962)], counterflow in a 0.14cm x 800cm metal circular channel.

C.E. Chase, Phys. Rev. **127**, 361 (1962), counterflow in a 0.08cm x 5.16cm metal circular channel.

P.E. Demotakis and J.E. Broadwell, Phys. Fluids **16**, 1787 (1973), counterflow in a 0.318cmX0.9cm glass circular channel.

R.K. Childers and J.T. Tough, Phys. Rev. B, **13**, 1040 (1976), couterflow in a 0.012cm x 10cm, 0.011cm x 10cm metal circular channel; 0.0126cm x 10cm, 0.0061cm x 10cm glass circular channel.

The experimental study of superfluid turbulence

D.R. Ladner and J.T. Tough, Phys. Rev. B, **17**, 1455 (1978); **20**, 2690 (1979); counterflow in a 0.098 x 0.0098 x 10 cm^3, 0.091 x 0.0091 x 10 cm^3, 0.047 x 0.0047 x 10 cm^3, 0.032 x 0.0032 cm^3 high-aspect-ratio rectangular glass channels and in a 0.0098cm x 10cm, 0.0091cm x 10cm, 0.0047cm x 10cm, 0.0032cm x 10cm narrow circular glass channel.

C.F. Barenghi, K. Park, and R.J. Donnelly, Phys. Lett. A, **84**, 435 (1981); counterflow in a 1.0 x 1.0 x 40 cm^3 wide, metal square channel.

L.B. Opatowsky and J.T. Tough, Phys. Rev. B, **24**, 5420 (1981); pure superflow in a 0.0057 x 0.057 x 9.4 cm^3 the high-aspect-ratio rectangular glass channel.

D.F. Brever and D.O. Edwards, J. Low Temp. Phys., **43** (1981), counterflow in a 0.00505cm x 10.2cm, 0.0368cm x 9.1cm circular glass channels.

R.A. Ashton, L.B. Opatowsky, and J.T. Tough, Phys. Rev. Lett. **46**, 658 (1981); pure superflow in a 0.013cm x 8cm circular glass channel.

J.D. Henberger and J.T. Tough, Phys. Rev. B **25**, 3123 (1982); counterflow in a 0.01 x 0.01 x 10cm^3 and in a 0.012 x 0.012 x 10 cm^3 narrow square glass channel.

The experimental study of superfluid turbulence

K.P. Martin and J.T. Tough, Phys. Rev. B **27**, 2788 (1983); counterflow in a 0.10 cm x 10 cm **circular** glass channel.

D.D. Awschalom, F.P. Milliken, and K.W. Schwarz, Phys. Rev. Lett. **53**, 1372 (1984); counter flow in a 1.0 x 2.3 x 26cm^3 wide metal rectangular channel.

D.J. Melotte and C.F. Barenghi, Phys. Rev. Lett. **80**, 4181 (1998).

T.V. Chagovets and L. Skrbek, Phys. Rev. Lett. **100**, 215302 (2008); J. Low Temp. Phys. **153**, 162 (2008); pure superflow in a 0.6 x 0.6 x 11.5cm^3, 1.0 x 1.0 x 11.5cm^3 square metal channel

S. Babuin, M. Stammeier, E. Varga, M. Rotter, and L. Skrbek, Phys. Rev. B **86,** 134515 (2012); pure superflow in a 0. 7 x 0.7 x 11.5cm^3 , 1.0 x 1.0 x 11.5cm^3 square metal channel.

A. Marakov, J. Gao, W. Guo, S.W. Van Sciver, G.G. Ihas, D.N. McKinsey, and W.F. Vinen, Phys. Rev. B **91,** 94503 (2015), counterflow in a 0.95 x 0.95 x 30 cm^3 square metal channel

Different states of superfluid turbulence

J.T. Tough, "Superfluid turbulence," in Progress in Low Temperature Physics (North-Holland Publ. Co., 1982), Vol. VIII.

Two states of turbulence (T-I --> T-II) are observed in small aspect ratio (circular or square) narrow tubes.
Only one state of turbulence T-III is observed in both wide and large aspect ratio (rectangular, approximately a parallel-plate geometry) channels in which the line density has essentially the same value as in *T*-II.

Schwarz's theory, unlike Vinen's, has no adjustable parameters and makes quantitative predictions about γ.

Note that the calculations were performed by Schwartz in the local-induced approximation. Besides, Schwartz used an artificial trick, the so-called "mixing" procedure, in which the vortices were rotated around the axis parallel to counterflow velocity randomly.

Tough found that Schwarz's gamma (K.W. Schwarz, Phys. Rev. Lett. **38**, 551 (1977); Phys.Rev. B **18**, 245 (1978); Phys. Rev. Lett. **49**, 283 (1982)) agrees fairly well to the measured values of gamma in the T-II state.

Comparison of experimental data with Schwarz' s calculations

K.P. Martin and J.T. Tough, Phys. Rev. B **27**, 1788, (1983)

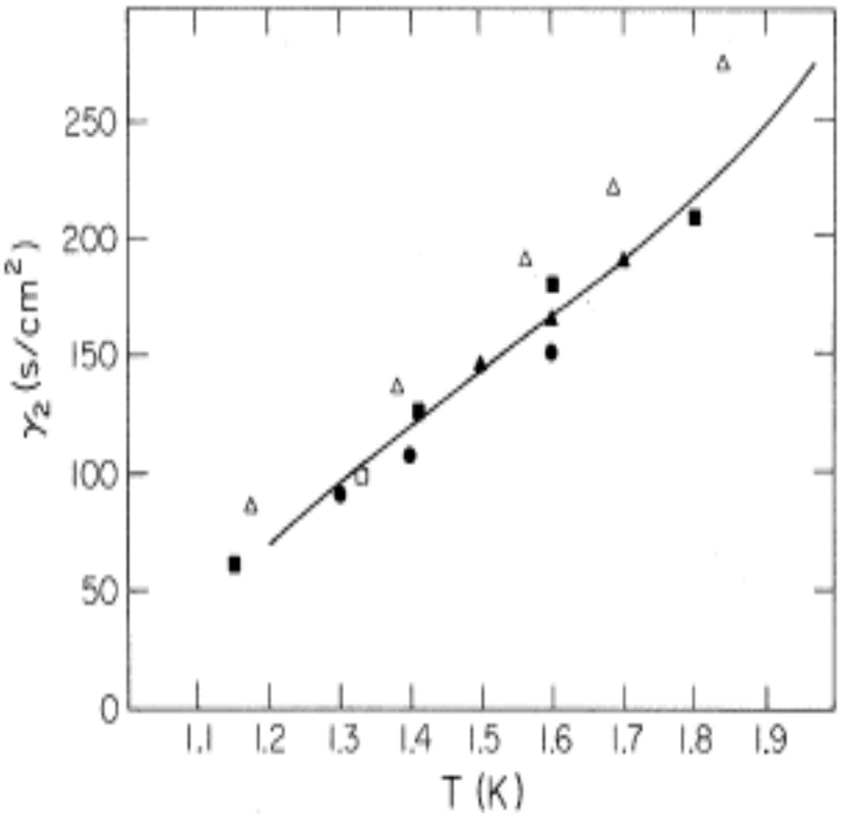

▲ K.P. Martin and J.T. Tough, Phys. Rev. B **27**, 2788 (1983); counterflow in a 0.10 cm x 10 cm circular glass channel

● P.E. Demotakis and J.E. Broadwell, Phys. Fluids **16**, 1787 (1973), counterflow in a 0.318cm x 0.9cm circular glass channel

□ V.P. Peshkov and V.J. Tkachenko, Zh. Eksp. Teor. Fiz. **41**, 1427 (1961) [Sov. Phys.-JETP 14, 1019 (1962)], counterflow in a 0.14cm x 800cm metal circular channel.

△ D.F. Brever and D.O. Edwards, J. Low Temp. Phys., **43** (1981), counterflow in a 0.00505cm x 10.2cm, 0.0368cm x 9.1cm circular glass channels.

▬ C.E. Chase, Phys. Rev. **127**, 361 (1962), counterflow in a 0.08cm x 5.16cm metal circular channel.

Solid line is the calculation of Schwarz for homogeneous turbulence.
K.W. Schwarz, Phys. Rev. Lett. **38**, 551 (1977); Phys. Rev. B **18**, 245 (1978); Phys. Rev. Lett. **49**, 283 (1982).

Comparison of experimental data with Schwarz' s calculations

D.D. Awschalom, F.P. Milliken, and K.W. Schwarz, Phys. Rev. Lett. **53**, 1372 (1984)

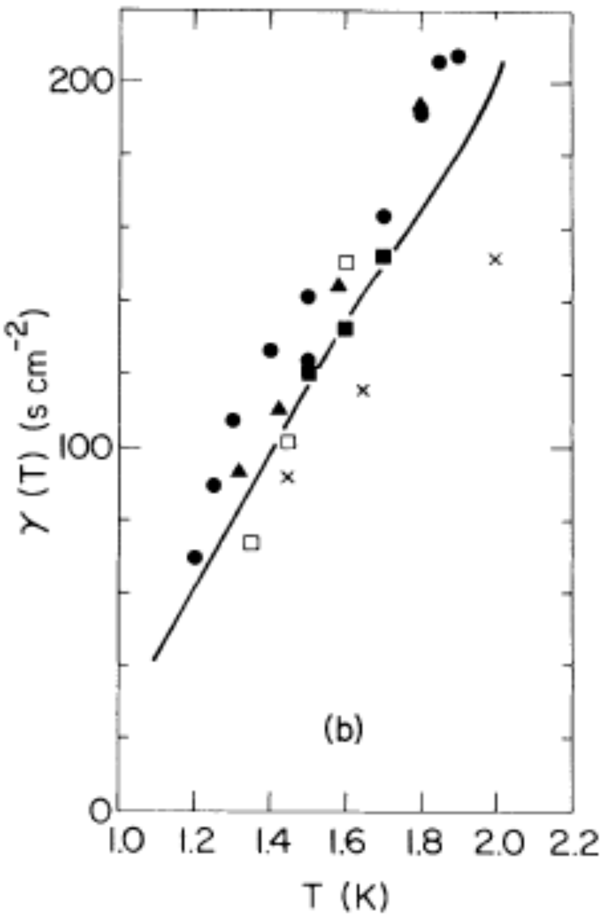

Triangles, W.F. Vinen, Proc. Roy. Soc. London, Ser. A **240**, 114 (1957), and **243**, 400 (1957); counterflow in a 0.4 x 0.78 x 10 cm^3 wide, low aspect-ratio rectangular metal channel.

"The crosses in Fig. are revised values from Barenghi's thesis, which differ considerably from the earlier published values." (C.F. Barenghi, K. Park, and R.J. Donnelly, Phys. Lett. A **84**, 435 (1981); counterflow in a 1.0 x 1.0 x 40 cm^3 wide, metal square channel.)

Open squares, D.D. Awschalom, F.P. Milliken, and K.W. Schwarz, Phys. Rev. Lett. **53**, 1372 (1984); counterflow in a 1 x 2.3 x 26cm^3 wide metal rectangular channel.

Squares, K.P. Martin and J.T. Tough, Phys. Rev. B **27**, 2788 (1983); counterflow in a 0.10 cm x 10 cm circular glass channel.

Circles, L.B. Opatowsky and J.T. Tough, Phys. Rev. B **24**, 5420 (1981); pure superflow in a 0.0057X0.057X 9.4 cm^3 the high-aspect-ratio rectangular glass channel.

Solid line is the calculation of Schwarz for homogeneous turbulence.

Note that the comparison was carried out with the experimental data obtained in the wide channels

Linear stability analysis of the Poiseuille normal flow

D.J. Melotte and C.F. Barenghi, Phys. Rev. Lett. **80**, 4181 (1998)

- Why are there two different kinds of superfluid vortex tangles : TI and TII? What is the nature of these tangles?

- What determines the critical velocity at which there is a transition from TI to TII with a dramatic increase of the superfluid vortex line density?

- Mellotte and Barenghi made linear stability analysis of the Poiseuille normal flow under the increasing forcing due to the tangle at higher and higher values of vortex line density.

- In the state TI: the superfluid is turbulent, the normal fluid is laminar.
- In the state TII: the superfluid is turbulent, the normal fluid is turbulent.

On flow of He II in channels with ends blocked by superleaks

S. Babuin, M. Stammeier, E. Varga, M. Rotter, and L. Skrbek, Phys. Rev. B **86**, 134515 (2012); pure superflow in a 0.7 x 0.7 x 11.5cm^3, 1.0 x 1.0 x 11.5cm^3 square metal channel (Flows are generated by mechanically operating a low temperature bellows assembly).

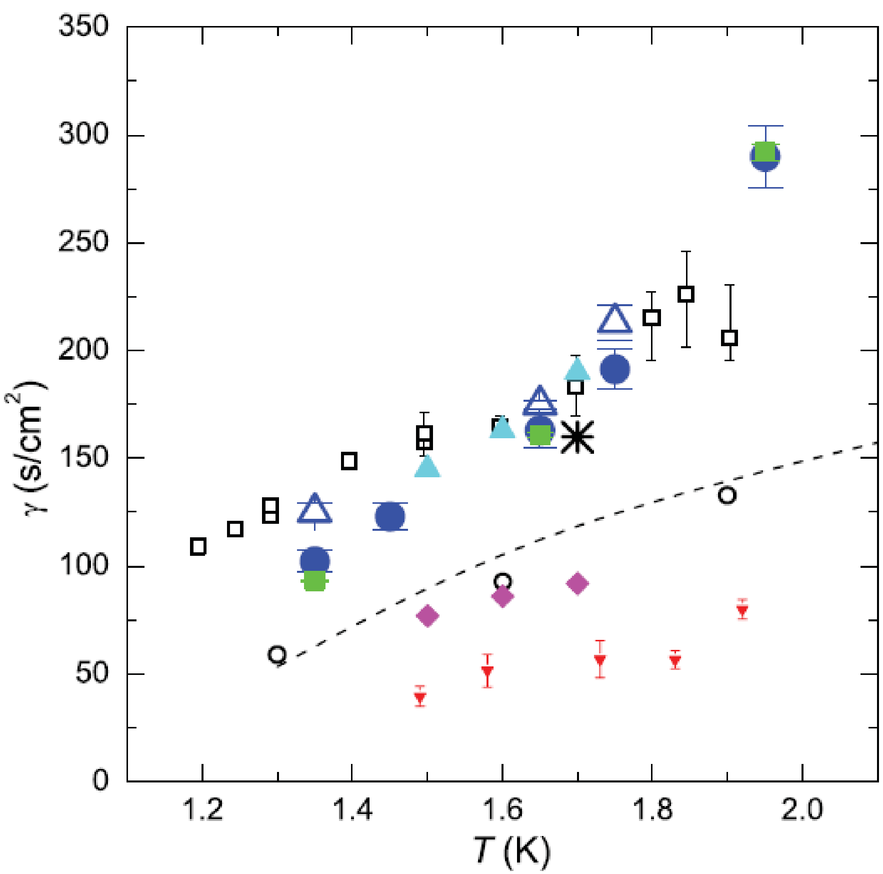

Present work:

solid blue circles, 0.7 cm channel;
solid green squares, 0.7 cm channel, downstream superleak removed;
open blue up-triangle, 1 cm channel.

Other works:

(i) thermally induced pure superflow,
open squares, R.A. Ashton, L.B. Opatowsky, and J.T. Tough, Phys. Rev. Lett. **46**, 658 (1981); pure superflow in a 0.013cm x 8cm circular glass channel;
solid red down-triangle, Chagovets and Skrbek, 0.7 cm
channel as present work, A-state turbulence;

(ii) counterflow,
solid blue up-triangle, solid magenta diamond, K.P. Martin and J.T. Tough, Phys. Rev. B **27**, 2788 (1983); counterflow in a 0.10 cm x 10 cm circular glass channel, TII and TI states;
open circles, R.K. Childers and J.T. Tough, Phys. Rev. B **13**, 1040 (1976), couterflow in a 0.0126cm x 10cm, 0.0061cm x 10cm glass circular channel, TI state;
asterisk, TII state, 0.7 cm channel as present work, unpublished
dashed line, H. Adachi, S. Fujiyama, and M. Tsubota, Phys. Rev. B **81**, 104511 (2010), numerical simulation.

Numerical simulations of superfluid turbulence

L. Kondaurova, V. L'vov, A. Pomyalov, and Itamar Procaccia,
Phys. Rev. B **89**, 014502 (2014). The vortex filament method

$$\frac{ds}{dt} = V_s + V_{BSE} + \alpha s' \times (V_{ns} - V_{BSE}) + \alpha' s' \times [s'(V_{ns} - V_{BSE})] + \vartheta_{bc}$$

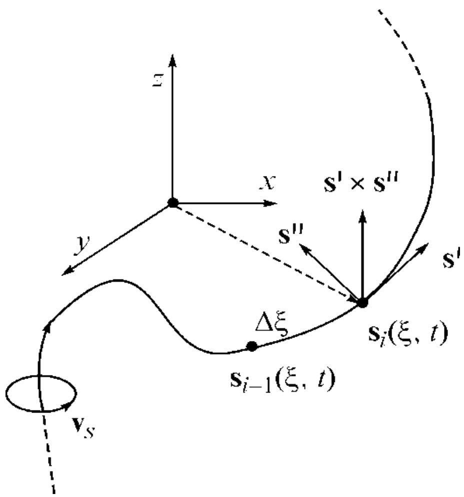

System of coordinates

$V_{ns} = V_n - V_s$ is the relative velocity between normal fluid and superfluid components

α, α' are the temperature-dependent friction coefficients

ϑ_{bc} is the boundary term

Biot-Savart law

$$V_{BSE}(s_i) = \beta s' \times s'' + \int_l \frac{(s_i - s_j) \times ds_j}{|s_i - s_j|^3}, \quad \beta = c\frac{\kappa}{4\pi}\ln\left(\frac{2(s_+ s_-)}{e^{1/4} a_0}\right)$$

$s_+ = s_{i+1} - s_i$, $\kappa = h / m_{^4He}$ is the quantum of circulation, a_0 is the vortex line core radius

$s_- = s_i - s_{i-1}$

The temperatures: T=1.3 K, T=1.6 K, T=1.9 K

The values of counterflow velocity: $V_{ns} = 0.3,\ 0.4,\ 0.5,\ 0.6,\ 0.7,\ 0.8,\ 0.9,\ 1.0,\ 1.1,\ 1.2\ (cm/s)$

Periodical boundary conditions are applied in all directions:

$\vec{V}_s(z) = \vec{V}_s(z + l_z),\ \vec{V}_s(x) = \vec{V}_s(x + l_x),\ \vec{V}_s(y) = \vec{V}_s(y + l_y)$ $\qquad l_z = l_x = l_y = 0.1\, cm$

Criteria of vortex reconnection

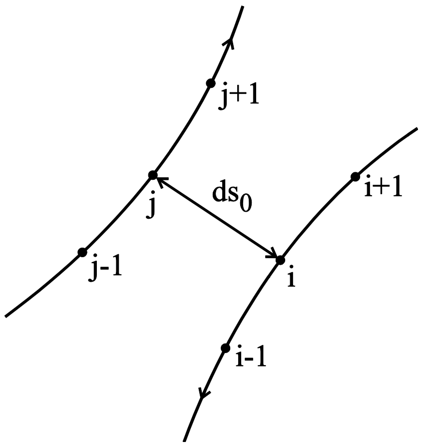

Geometry based:

G : reconnect, if two points come closer than the inter-point distance ds_0, without any additional restrictions.

M. Tsubota, T. Araki, and S.K. Nemirovskii, Phys. Rev. B **62**, 751(2000)

GE criterion is similar to G , with additional requirement that the reconnection only takes place if the total length is reduced upon reconnection.

M. Leadbeater, T. Winiecki, D.C. Samuels, C.F. Barenghi, and C.S. Adams, Phys. Rev. Lett. **86**, 1410 (2001)
R. Tebbs, A.J. Youd, and C.F. Barenghi, J. Low Temp. Phys. **162**, 314 (2010)

Dynamics based:

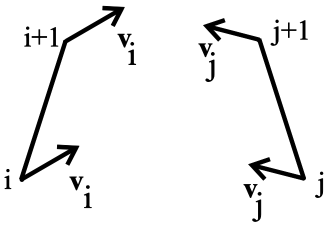

D : reconnect, if the segments will intersect in space during next time step.

L.P. Kondaurova, S.K. Nemirovskii, J. Low Temp. Phys.**138**, 555 (2005)

Statistical properties of the vortex tangle

⇨ The line density as a function of time: $L(t) = (1/V)\int_l ds$

⇨ The mean density of the tangle in the equilibrium: $\langle L \rangle$

The mean density is related to other properties

⇨ The counterflow velocity: $\langle L \rangle = \gamma^2 V_{ns}^2$

⇨ The intervortex distance: $\delta = 1/\sqrt{\langle L \rangle}$

⇨ The mean second derivative and its square: $\langle |s''| \rangle = c_1 \langle L \rangle^{1/2}, \quad \langle |s''|^2 \rangle = c_2^2 \langle L \rangle$

⇨ The mean reconnection rate in the steady state: $\left\langle \frac{dN_r}{dt} \right\rangle = c_r \kappa \langle L \rangle^{5/2}$

M. Tsubota, T. Araki, and S.K. Nemirovskii, Phys. Rev. B **62**, 751(2000),
C.F. Barenghi, D.C. Samuels, JLTP **156**, 281 (2004),
L.P. Kondaurova, V.A. Andryuschenko, S.K. Nemirovskii, JLTP **150**, 415 (2008).

⇨ Drift velocity of the vortex tangle V_{vt} and parameter C_{vt}

$$\mathbf{V}_{\rm vt} = \frac{1}{L_{\rm tot}} \int_C \frac{d\mathbf{s}(\xi)}{dt} d\xi - \mathbf{v}_s, \quad \mathbf{V}_{\rm vt} = C_{\rm vt} \mathbf{v}_{\rm ns}$$

L. Kondaurova, V. L'vov, A. Pomyalov, and Itamar Procaccia, Phys. Rev. B **89**, 014502 (2014)

Statistical properties of the vortex tangle

- The anisotropy indexes of the tangle: $I_{II} = \frac{1}{VL}\int [1-(s'\cdot\hat{r}_{II})^2]\, d\xi,$

K.W. Schwarz, Phys. Rev. B **38**, 2398 (1988).

$$I_{\perp} = \frac{1}{VL}\int [1-(s'\cdot\hat{r}_{\perp})^2]\, d\xi, \quad I_l = \frac{l}{L_{tot}}\int_C \hat{r}_{II}\cdot(s'\times s'')d\xi, \quad I_{l\perp} = \frac{l}{L_{tot}}\int_C \hat{r}_{\perp}\cdot(s'\times s'')d\xi, \quad l = 1/\sqrt{L}$$

- Autocorrelation of the vortex orientations $K(\mathbf{r}_1-\mathbf{r}_2) = \langle \mathbf{s}'(\mathbf{r}_1)\cdot\mathbf{s}'(\mathbf{r}_2)\rangle_C$
- Friction force density and the Gorter-Mellink constant

$$\mathbf{F}_{ns} = \rho_s \kappa \alpha \mathbf{J}, \;\; \mathbf{J} = -\frac{1}{v}\int_C \mathbf{s}'\times[\mathbf{s}'\times(\mathbf{v}_{ns}-\mathbf{v}_{BSE})]d\xi, \quad F_{sn} = A_{GM}\rho_s\rho_n \mathrm{v}_{ns}^3$$

- Probability density function (PDF) of vortex-loop lengths
- PDF of the line curvature
- Correlation between loop length and root-mean-square (RMS) of the loop curvature
- PDFs of the mean and RMS the loop curvature

L. Kondaurova, V. L'vov, A. Pomyalov, and Itamar Procaccia, Phys. Rev. B **89**, 014502 (2014)

Comparison of experimental data with calculations

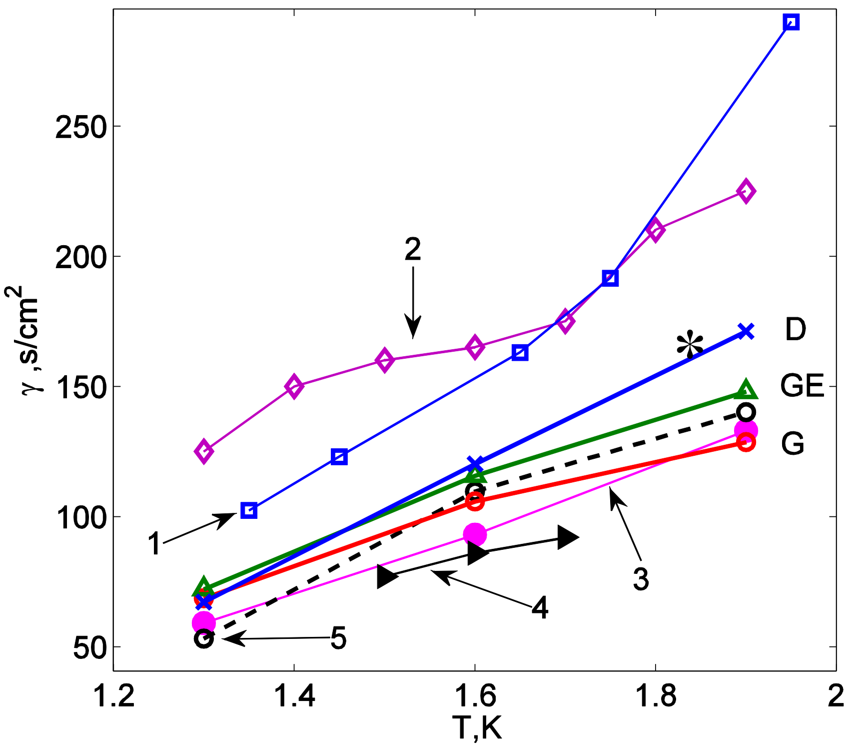

Experimets:

1 - V_n =0, S. S. Babuin, M. Stammeier, E. Varga, M. Rotter, and L. Skrbek, Phys. Rev. B **86**, 134515 (2012); pure superflow in a 0.7 x 0.7 x 11.5 cm^3, 1.0 x 1.0 x 11.5 cm^3 square metal channel;

2 - R.A. Ashton, L.B. Opatowsky, and J.T. Tough, Phys. Rev. Lett. **46**, 658 (1981); pure superflow in a 0.013cm x 8cm circular glass channel;

3 - R.K. Childers and J.T. Tough, Phys. Rev. B **13**, 1040 (1976), couterflow in a 0.0126cm x 10cm glass circular channel R.K. Childers and J.T. Tough, Phys. Rev. B, **13**, 1040 (1976), couterflow in a 0.012cm x 10cm, 0.011cm x 10cm metal circular channel; 0.0126cm x 10cm, 0.0061cm x 10cm glass circular channel;

4 - K.P. Martin and J.T. Tough, Phys. Rev. B **27**, 2788 (1983); counterflow in a 0.10 cm x 10 cm circular glass channel;

Simulation:

5 - H. Adachi, S. Fujiyama, and M. Tsubota, Phys. Rev. B **81**, 104511 (2010)

* A. Marakov, J. Gao, W. Guo, S.W. Van Sciver, G.G. Ihas, D.N. McKinsey, and W.F. Vinen Phys. Rev. B **91**, 94503 (2015), superflow in a 0.95 x 0.95 x 30 cm^3 square metal channel, T = 1.83 K, γ = 162s/cm^2.

The transition to normal fluid turbulence around 80 mW/cm^2 , $V_{ns} \approx 0.766$ cm/s

Comparison of calculations of ɣ

	Recon. criterion	$T = 1.3$ K	$T = 1.6$ K	$T = 1.9$ K
	GC	68.6 ± 0.1	105.8 ± 0.2	128.6 ± 0.7
γ, s/cm^2	GEC	72.1 ± 0.2	115.7 ± 0.1	148.0 ± 0.2
	DC	67.1 ± 0.4	120.2 ± 0.7	171.2 ± 2.6
$\Gamma \simeq$	GEC	0.07	0.12	0.15
	GC	3.1 ± 0.1	-0.8 ± 0.1	-5.4 ± 0.3
$10^2 v_0$, cm/s	GEC	6.6 ± 0.3	3.3 ± 0.1	0.2 ± 0.1
	DC	1.6 ± 0.4	4.3 ± 0.5	4.3 ± 0.4
γ, Ref. [22]	GC	53.1	109.6	140.1
	GC		116.9	
γ, Ref. [52]	GE		114.35	
	DC		112.3	
γ_V, Eq. (18)		82	151	266
γ_S, Eq. (19)	Ref. [19]	80	130	198

22. H. Adachi, S. Fujiyama, and M. Tsubota, Phys. Rev. B **81**, 104511 (2010).
52. A. Baggaley, J. Low Temp. Phys. **168**, 18 (2012).

$$\gamma_V = \frac{\pi B \rho_n \chi_1}{\kappa \rho \chi_2}$$

$$\gamma_S = c_L/\beta, \quad c_L \equiv I_\ell / c_2^2.$$

$$I_\ell = \frac{\ell}{L_{tot}} \int_C \hat{r}_\parallel \cdot (s' \times s'') d\xi$$

A. W. Baggaley and S. Laurie, J. Low Temp. Phys. **178**, 35 (2014)
ɣ = 157 s/cm^2 (T= 1.6 K), ɣ = 195 s/cm^2 (T = 1.9 K) - the simulation for turbulent normal fluid between parallel plates
ɣ = 83.6 s/cm^2 (T = 1.6 K), ɣ = 105,7 s/cm^2 (T = 1.9 K) – simulation for Poiseuille flow between parallel plates, vortex filament method ↔ Navier-Stoces equations

S. Yui and M. Tsubota, Phys. Rev. B **91**, 184504 (2015)
ɣ = 31 s/cm^2 (T = 1.3 K), ɣ = 47 s/cm^2 (T = 1.6 K), ɣ = 103 s/cm^2 (T = 1.9 K) simulation for Hagen-Poiseuille flow in square channel ; ɣ = 176 s/cm^2 (T = 1.9 K) - tail-flat h=0.7

Summary

- In the state TII (circular or square narrow tubes), wide low-aspect-ratio rectangular, large aspect ratio (rectangular, approximately a parallel-plate geometry) channels, pure superflow have the same value of ɣ.

- Schwarz's gamma (simulations by using of the vortex filament method in local-induced approximation) at constant of V_{ns} and the simulations for turbulent normal fluid between parallel plates (simulations by the vortex filament method with using full Biot-Savart equation↔ Navier-Stoces equations) agree fairly well to the measured these experimental values of ɣ . Normal fluid is turbulent.

- In the state TI (circular or square narrow tubes) normal fluid is laminar.

- Simulations by the vortex filament method with using full Biot-Savart equation at constant of V_{ns} and simulations for Poiseuille flow between parallel plates (vortex filament method ↔ Navier-Stoces equations) agree closely with the measured experimental values of ɣ in the state TI.
- **Simulations for Hagen-Poiseuille flow in** square channel give lower ɣ.

- **Simulations at** tail-flat h=0.7 give, however, the value of ɣ seems to be too large

What is the structure of the vortex tangle in different channels at different values V_{ns}?
What is the correct equation for the evolution of the density of the vortex tangle?